Heterotypic Docking of Cx43 and Cx45 Connexons Blocks Fast Voltage Gating of Cx43

Sergio Elenes,* Agustin D. Martinez,† Mario Delmar,‡ Eric C. Beyer,† and Alonso P. Moreno*
*Krannert Institute of Cardiology, Indiana University, Indianapolis, Indiana 46202; †Department of Pediatrics, University of Chicago, Chicago, Illinois 60637; and ‡Department of Pharmacology, State University of New York Upstate Medical University, Syracuse, New York USA

ABSTRACT Immunohistochemical co-localization of distinct connexins (Cxs) in junctional areas suggests the formation of heteromultimeric channels. To determine the docking effects of the heterotypic combination of Cx43 and Cx45 on the voltage-gating properties of their channels, we transfected DNA encoding Cx43 or Cx45 into N2A neuroblastoma or HeLa cells. Using a double whole-cell voltage-clamp technique, we determined macroscopic and single-channel gating properties of the intercellular channels formed. Cx43-Cx45 heterotypic channels had rectifying properties where Cx45 connexons inactivated rapidly upon hyperpolarizing voltage pulses applied to the Cx45-expressing cell. During depolarizing pulses to the Cx45-expressing cell, Cx43 connexons inactivated with substantially reduced kinetics as compared with homotypic Cx43 channels. Similar slow kinetics was observed for homotypic Cx43M257 (truncation mutant). Heterotypic channels had a main conductance whose value was predicted by the sum of corresponding homomeric connexon conductances; it was not voltage dependent and had no detectable residual conductance. The voltage-gating kinetics of heterotypic channels and their single-channel behavior implicate a role for the Cx43 carboxyl-terminal domain in the fast gating mechanism and in the establishment of residual conductance. Our results also suggest that heterotypic docking may lead to conformational changes that inhibit this action of the Cx43 carboxyl-terminal domain.

INTRODUCTION

Gap junctions contain intercellular channels that allow communication between adjacent cells. Connexins constitute a homologous family of gap junction proteins. A connexon (or hemichannel) is formed by the oligomerization of six connexin subunits, and the assembly and docking of two connexons leads to the formation of a complete gap junction channel.

Multiple connexins are expressed in the mammalian heart and many other organs (Kanter et al., 1993; Gros and Jongsma, 1996; Coppen et al., 1998). Using specific antibodies, connexin43 (Cx43), connexin40 (Cx40), and connexin45 (Cx45) have been detected in the working myocardium. Other connexins have also been described in this organ, but their expression either is restricted to endothelial cells (Cx37) (Reed et al., 1993; Haefliger et al., 2000) or only their mRNA has been identified in the heart (Cx46) (Paul et al., 1991).

The co-existence of connexins in tissue indicates that channels could be assembled with more than one type of connexin. A complete new nomenclature for the different possible configurations has already been generated (Wang and Peracchia, 1998). The most relevant issue for channels formed of different connexins is that each one could provide the channels with different gating and permeability properties. Therefore, the interactions between these isoforms could result in channels with highly complex gating mechanisms. To fully understand the outcome of these interactions, it has been necessary to use simple cellular systems in which the expression and assembly of hemichannels among different cells can be controlled. One of the simplest configurations where connexin interaction can be studied is the heterotypic channel, which results from the assembly of two different homomeric hemichannels (Fig. 1).

In this manuscript, we have further characterized the effects of heterotypic docking between Cx43 and Cx45 on gating produced by transjunctional voltage. Despite the homology of connexin sequences, strong differences exist in their gating and permeability properties. The channels formed by these connexins are sensitive to transjunctional voltage, as shown in studies performed in cellular systems that permit the expression of exogenous genes, such as *Xenopus* oocytes (Werner et al., 1989; Steiner and Ebihara, 1996) or transfected cells (Moreno et al., 1995a,b). The use of transfected cells has several advantages over *Xenopus* oocyte expression, including possible differences in behavior of mammalian connexins expressed in non-mammalian cells. Besides, transfection of cDNA into communication-deficient tumor cell lines has become a standard procedure (Moreno et al., 1991) that allows single-channel recordings, necessary to elaborate a complete gating model of these mammalian connexins.

For our studies, we stably transfected cloned cDNAs for rat Cx43 (rCx43) (Beyer et al., 1987), chicken Cx45 (chCx45) (Beyer, 1990), or mouse Cx45 (mCx45) (Hennemann et al., 1992) in two different tumor cell lines: HeLa and neuroblastoma N2A. Having ascertained the individual gating behavior and unitary conductances for the channels containing only Cx43 or Cx45, we then

Received for publication 10 October 2000 and in final form 7 June 2001.
Address reprint requests to Dr. Alonso P. Moreno, Krannert Institute of Cardiology, 1111 West 10th Street, Indianapolis, IN 46202. Tel.: 317-630-6051; Fax: 317-630-7776; E-mail: amoreno@iupui.edu.

0006-3495/01/09/1406/13 $2.00

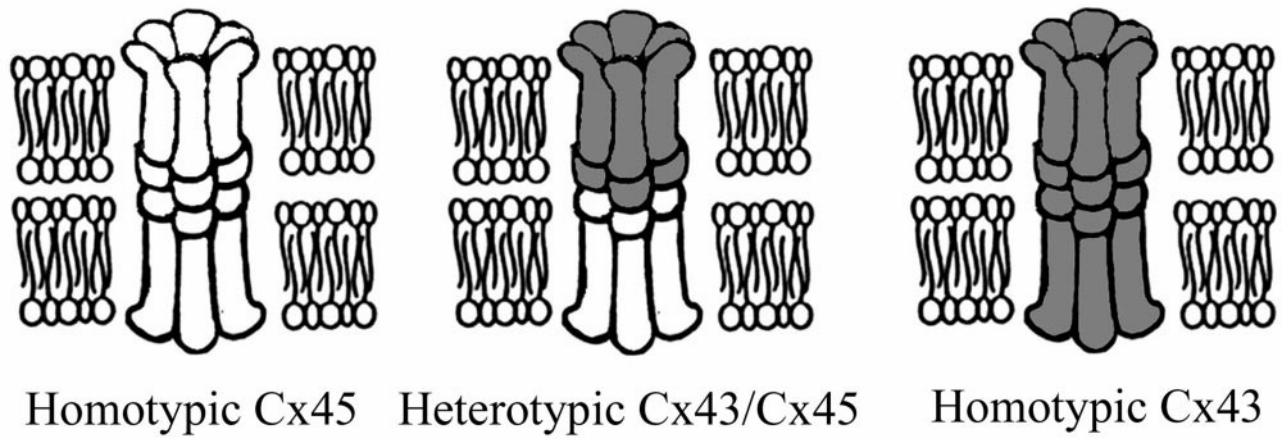

FIGURE 1 Cx45 and Cx43 forming homotypic and/or heterotypic channels. In the current study, we have considered only gap junction channels where an entire connexon (hemichannel) contains only one kind of connexin (homomeric connexons). Such homomeric connexons can pair with themselves to form homotypic channels (*right* and *left panels*) or they could pair with connexons formed of a different connexin forming heterotypic channels (*center panel*). The additional possible formation of heteromeric connexons containing multiple connexins (not illustrated) might occur in cells co-expressing multiple connexins.

performed studies on cell pairs that were forced to form heterotypic channels. To determine whether opposite gating polarities of Cx43 and Cx45 were responsible for the observed behaviors, we performed studies on heterotypic channels formed by wild-type Cx43 and Cx43M257, a mutant of Cx43 that is insensitive to pH gating (Ek-Vitorin et al., 1996) and lacks the fast component of voltage-dependent inactivation (Revilla et al., 1999).

Our data provide evidence that the heterotypic combination of homomeric Cx43 and Cx45 connexons generates channels with complex behavior, where the voltage-gating mechanism of Cx43 becomes impaired after docking, and the residual conductance of the channels is no longer detectable. The data also imply that connexon interaction participates in the modulation of intercellular communication.

MATERIALS AND METHODS

Cells in culture and transfection

HeLa cells and mouse (Neuro2a, N2A) neuroblastoma cells were obtained from American Type Culture Collection (ATCC, Rockville, MD) and were cultured in tissue culture medium (Dulbecco's minimal essential medium; GIBCO/BRL, Gaithersburg, MD) containing 10% fetal bovine serum (GIBCO/BRL) at 37°C in CO_2-controlled incubators. These cell lines have been extensively used for gap junction channel expression (Veenstra et al., 1992, 1995; Traub et al., 1994). N2A cells were transfected with cDNA sequences encoding mCx45 or rCx43 that had been subcloned into pCDNA3.1 (Invitrogen, Chatsworth, CA). N2A cells were transfected with 6 μg of plasmid DNA using the LipofectAmine reagent (GIBCO/BRL), and stable clones were selected in medium containing G418 (0.5–1.0 mg/ml; GIBCO/BRL). HeLa cells were similarly transfected with the pSFV-neo plasmid containing either rCx43 or chCx45 cDNAs as described previously (Veenstra et al., 1992). N2A cells expressing Cx43M257 were provided by Dr. Steve Taffet (Syracuse, NY).

Heterotypic gap junction channels were induced after co-plating individual cells expressing Cx43 channels with those expressing Cx45 or Cx43M257. To identify heterotypic pairs, cells expressing Cx43 were stained with a red fluorescent dye (DiI; Molecular Probes, Eugene, OR; 100 μM for 60 min at 37°C).

Immunoblotting

Samples of parental or stably transfected HeLa and N2A cells were prepared for immunoblotting. Cell cultures were rinsed with PBS (pH 7.4) and then harvested in ice-cold 2 mM phenylmethylsulfonyl fluoride (PMSF) in PBS. The cell suspensions were centrifuged, the supernatant was discarded, and cell pellets were frozen in liquid nitrogen and stored at −80°C. Cell pellets were resuspended in water containing protease inhibitors (200 g/ml soybean trypsin inhibitor, 1 mg/ml benzamidine, 1 mg/ml β-aminocaproic acid, and 2 mM PMSF) and phosphatase inhibitors (20 mM $Na_4P_2O_7$ and 100 mM NaF) and lysed by sonication. The protein concentrations of cell homogenates were determined using the method of Bradford (1976) (Bio-Rad, Richmond, CA). In some experiments, we prepared a fraction enriched in gap junction plaques using alkali extraction. Briefly, 1 ml of $NaHCO_3$ containing protease and phosphatase inhibitors and 22 μl of 1 M NaOH were added to frozen cell pellets. This cell suspension was sonicated for 30 s and incubated on ice for 50 min. Then, the homogenate was centrifuged for 30 min at 30,000 $\times$ g at 4°C. The supernatant was discarded, and the pellet was resuspended in sample buffer.

Western blot analyses were performed essentially as described previously (Berthoud et al., 2000). Protein samples (100 μg) were resolved on 8% polyacrylamide gels containing sodium dodecyl sulfate (SDS-PAGE). Proteins were electro-transferred from gels onto Immobilon-P membranes (Millipore, Bedford, MA) at 300 mA for 1.5 h. Membranes were incubated in 5% nonfat milk in Tris-buffered saline (TBS), pH 7.4, overnight at 4°C, and then incubated with mouse monoclonal anti-Cx43 or anti-Cx45 antibodies (Chemicon, Temecula, CA) diluted in 5% nonfat milk in TBS for 3 h at room temperature. Membranes were rinsed repeatedly in TBS and then incubated for 30 min at room temperature with horseradish-peroxidase-conjugated secondary goat anti-mouse antibodies (Jackson ImmunoResearch, West Grove, PA). After rinsing repeatedly in TBS, the antibody binding was detected by chemi-

luminescence (ECL, Amersham, Arlington Heights, IL) followed by exposure to x-ray film.

Electrophysiology

A dual whole-cell voltage-clamp technique was applied to measure the junctional conductance (g_j) between cells. Access to the cytoplasm was achieved by using a brief negative-pressure pulse after a gigaohm seal was formed between polished glass micropipettes (3–5 MOhm) and the cell membrane. The micropipettes were filled with a cesium-chloride-containing patch solution (in mM: 130 CsCl, 0.5 $CaCl_2$, 10 Hepes, 10 tetraethylammonium chloride, 10 EGTA, pH 7.0). During recording, cells were kept at room temperature in cesium-containing bathing solution (in mM: 160 NaCl, 7 CsCl, 2.0 $CaCl_2$, 0.6 $MgCl_2$, 10 Hepes, pH 7.4). The voltage sensitivity of junctional channels was determined by measuring the transjunctional current (i_j) in one of the cells (held at constant voltage), while a computer-driven protocol consisting of voltage steps (ranging from −100 to 100 mV, incrementing by 10 or 20 mV) was applied to the partner cell (pClamp6 software; Axon Instruments, Foster City, CA). All current traces were digitized (NeuroCorder, NeuroData Instruments Corp., New York, NY) and stored on VCR tapes. The series resistance was compensated in all experiments up to 70%. The initial current (i_i) was measured at the beginning of the voltage pulses using a low-pass filter of 5 kHz.

All macroscopic voltage-dependent current traces were digitized at 11 kHz and acquired at 1 kHz for analysis. To avoid under-sampling in the fast inactivation of Cx45 channels, the first 100 ms of the traces were filtered at 5 kHz and acquired at 10 kHz. The steady-state current (i_{ss}) was obtained 10 s after the initiation of the pulse. The initial conductance (g_i) and the steady-state conductance (g_{ss}) for each pulse were then calculated as ratios of the currents to the transjunctional voltages: i_{inst}/V_j and i_{ss}/V_j. The steady-state voltage sensitivity (G_{ss}-V_j) of gap junction channels was obtained after normalization to a hyperpolarizing 5-mV pre-pulse of 200 ms. The current traces of all the experiments were scaled to the average conductance value obtained during the test pulses. Voltage dependence was analyzed using an equation that allows the simultaneous fitting at both polarities (Chen et al., 2001):

$$G_{ss} = G_{min} + \frac{G_{max} - G_{min}}{(1 + e^{A1(-V-V01)})(1 + e^{A2(V-V02)})}$$

This equation has six parameters. G_{max} and G_{min} are assigned to obtain the maximal and minimal conductance; A_1 and A_2 are constants for each connexon where A equals nq/kT and reflects the voltage sensitivity of the transitions between two conductive states. Vo_1 and Vo_2 indicate the voltage, for each connexon, at which the initial conductance reaches half of its value. Equation 1 allows us to simultaneously obtain voltage-dependent parameters for each of the connexons in the junction.

Single-channel currents were measured either by using freshly split cells, where junctional conductance was low or after macroscopic conductance was reduced by superfusing the cells with an external solution containing 2 mM halothane (Burt and Spray, 1989). Amplitudes of unitary opening or closing current events were measured using a digitizing board (Summagraphics with SigmaScan software; Jandel, Corta Madera, CA) from the chart recorder paper (Gould Instruments Systems, Valley View, OH) where current traces were filtered at 100–500 Hz. Frequency distribution histograms of the events using Origin software (Originlab Corporation, Northampton, MA) and Gaussian distribution best fits were calculated for each experiment (Origin). Each event was defined as the current transition between channel states, where the residence time in each state was longer than 20 ms. The nonlinear regression method used for least-squares fitting is based on the Levenberg-Marquardt (LM) algorithm. This algorithm minimizes χ^2 by performing a series of iterations on the initial parameter values and computes χ^2 at each stage. For this process, the computer program internally calculates partial derivatives for all the values of the input variables. All-point histograms were generated using pClamp protocols from traces filtered at 200–500 Hz and digitized at 1 kHz. Digitized points were grouped into 128 points/bin. Multiple Gaussian functions were also obtained by following the LM algorithm to determine the best bell-shaped curves for normal (Gaussian) probability distribution functions. Inactivation time constants for macroscopic currents were calculated using single- or double-exponential fittings (Origin). Unitary junctional currents were also recorded during 10-s voltage ramps applied to one of the cells. Here, the unitary conductance was calculated using the slopes of the digitized junctional current traces imported into Origin.

RESULTS

Expression of connexins: Western blots

The expression of Cx45 and Cx43 in parental and stably transfected HeLa or N2A cells was examined by immunoblotting using connexin-specific antibodies. Parental (wild-type, WT) N2A cells did not contain detectable levels of either Cx45 or Cx43 protein (Fig. 2, *A* and *B*, *lanes 1*). Similarly, no Cx43 protein was detected in WT HeLa cells (Fig. 2 *B*, *lane 3*). No Cx45 protein was detected in PBS extracts of WT HeLa cells (not shown), but when WT HeLa cell extracts were concentrated by alkali extraction, Cx45 protein was detected. Cx45 was detected only in N2A cells transfected with mCx45 (Fig. 2 *A*, *lane 2*). HeLa cells transfected with chCx45 (Fig. 2 *A*, *lane 4*) showed a significant increase in Cx45 expression, compared with that of WT HeLa cells. Both N2A and HeLa cells transfected with rCx43 (Fig. 2 *B*, *lanes 2* and *4*) produced Cx43 protein. The levels of both Cx45 and Cx43 appeared to be higher in the HeLa cell transfectants than in the N2A cells. This correlated with a higher conductance between cells (not shown). Immunoblots also suggested that the modification of both Cx45 and Cx43 differed between N2A and HeLa transfectants with slower mobility bands more prominent in HeLa cells. Many previous studies of Cx43 have correlated such electrophoretic mobility variants with differences in connexin phosphorylation (Musil et al., 1990; Crow et al., 1990). Overall, these results confirm production of appropriate connexins in the transfected cells.

Macroscopic current measurements from homotypic channels

Homotypic rCx43 macroscopic currents

At a macroscopic level, junctional currents in pairs of cells expressing Cx43 were inactivated when transjunctional voltages from −100 to +100 mV were applied; after several seconds, they reached a steady state (Fig. 3 *A*). The data from both N2A and HeLa transfectants at the bottom (closed and open symbols, respectively) show that G_i was not significantly affected by voltage, whereas G_{ss} declined for V_j values larger than 20 mV. The continuous line depicts the best fit using Eq. 1 with the parameters shown in Table 1.

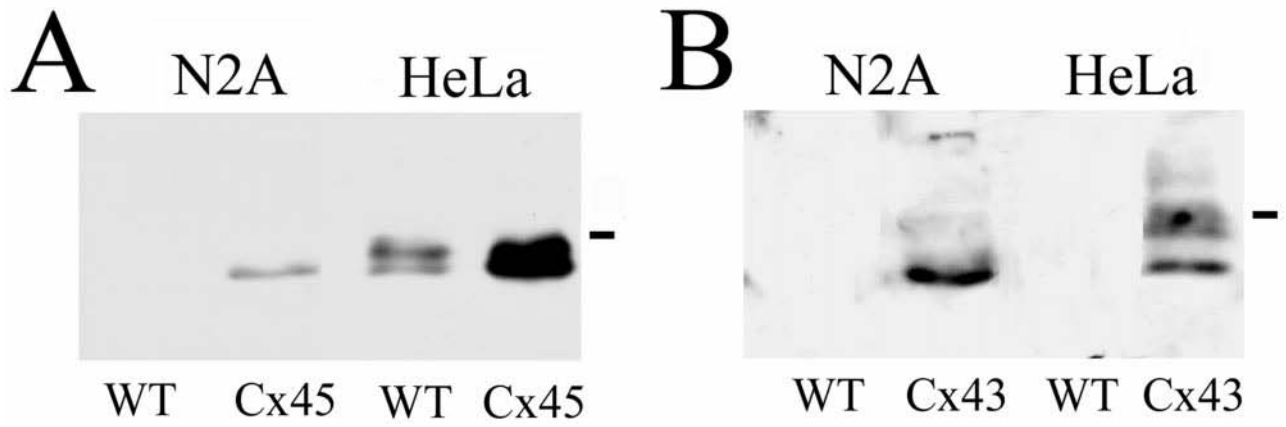

FIGURE 2 Immunoblot detection of Cx43 and Cx45 in transfected cells. Parental (wild-type, WT) N2A or HeLa cells and cells stably transfected with Cx45 or Cx43 (indicated above and below each panel) were cultured, and extracts containing gap junctions were prepared by alkali extraction (as described in Materials and Methods). (*A*) Blot reacted with anti-Cx45 antibodie; (*B*) Blot reacted with anti-Cx43 antibodies. The migration of a 46-kDa standard protein (ovalbumin) is indicated to the right of each panel. The data shown confirm the production of Cx45 protein in N2A/mCx45 cells and HeLa/chCx45 cells (as well as WT HeLa cells) and the production of Cx43 in N2A/rCx43 and HeLa/rCx43 cells.

Homotypic mCx45 macroscopic currents

Various nonstable clones were obtained after transfection of mCx45 into N2A cells. One of the N2A clones averaged 50 channels (~2 nS; $n = 10$), and other clones demonstrated between 5 and 10 channels per pair (~0.4 nS; $n = 20$). We took advantage of these differences to analyze either macroscopic voltage dependence using high-expressing clones or single-channel currents using clones with lower levels of expression. Those clones from stable transfections in HeLa cells were consistently better coupled (~5–10 nS) than those from N2A cells.

Gap junctional channels in cells expressing Cx45 were found to be highly sensitive to transjunctional and transmembrane voltages (Fig. 3 *B*), as previously reported (Elenes and Moreno, 1998; Barrio et al., 1997). In both N2A and HeLa cells, the initial current decreased rapidly with voltage pulses of either polarity, reaching a steady-state value at ~10% of initial current (Fig. 3 *B*, *middle panels*). The voltage/conductance relationship is shown at the bottom of Fig. 3 *B*. With transjunctional voltage gradients larger than 20 mV, the steady-state current significantly decreased, reaching the lowest values at −80 mV. The rapid decrease in initial conductance (G_i) was larger than that observed for homotypic rCx43 channels (Fig. 3 *A*), which was reduced 80% at ±100 mV. Gating to transjunctional voltage was symmetric around zero mV. All parameters for the best fit for Eq. 1 are presented in Table 1.

Heterotypic rCx43-mCx45 macroscopic currents

The rectifying properties of heterotypic junctions formed by homomeric rCx43 and mCx45 in N2A and HeLa cells were confirmed by co-plating cells expressing each of the two connexins for each cell type, respectively. When the cell that expressed mCx45 was pulsed to negative voltages, the initial transjunctional conductance (g_i) was strongly affected, decreasing by 40% at −100mV (Fig. 3 *C*). This change was significantly larger than that for homotypic mCx45 channels (Fig. 3 *B*). Junctional current declined rapidly, reaching steady-state (g_{ss}) values close to zero at −100 mV. Depolarizing pulses to the Cx45-expressing cell also induced instantaneous reduction in G_i (a 10% decrease from the initial current value). Thereafter, the inactivation kinetics for Cx43 connexons heterotypically paired with Cx45 ($Cx43_{hetCx45}$) did not resemble those of homotypic rCx43; here, inactivation occurred with a substantially longer and single time constant (see Fig. 3 *C*). The best fit for conductances at steady state was obtained using Eq. 1 for heterotypic channels. The voltage-gating behavior of Cx45-Cx43 heterotypic channels was also studied in HeLa cell pairs expressing chCx45 and rCx43. These transjunctional currents are shown under the N2A traces. G_i and G_{ss} were also plotted on the bottom panels for homotypic and heterotypic channels and are shown by open symbols. In short, the expression of rat Cx43 and chicken Cx45 in HeLa cells yielded heterotypic channels with similar gating properties to those obtained from N2A cells.

The changes in voltage-gating kinetics were compared by examining a set of traces obtained from five N2A cell pairs ($V_j = \pm 80$ mV; Fig. 4 *A*). Even though the current traces appeared very similar for Cx45 connexons in both homomeric and heterotypic configurations (Fig. 4 *A*), it is clear that a steady state is not reached in heterotypic channels before the current decays to zero. The fast inactivation time constants (τ_1) determined for mCx45 connexons in homotypic mCx45-mCx45 or heterotypic mCx45-rCx43 channels were also similar when determined at various voltages (Fig. 4 *B*), although the slower time constant (τ_2) was signifi-

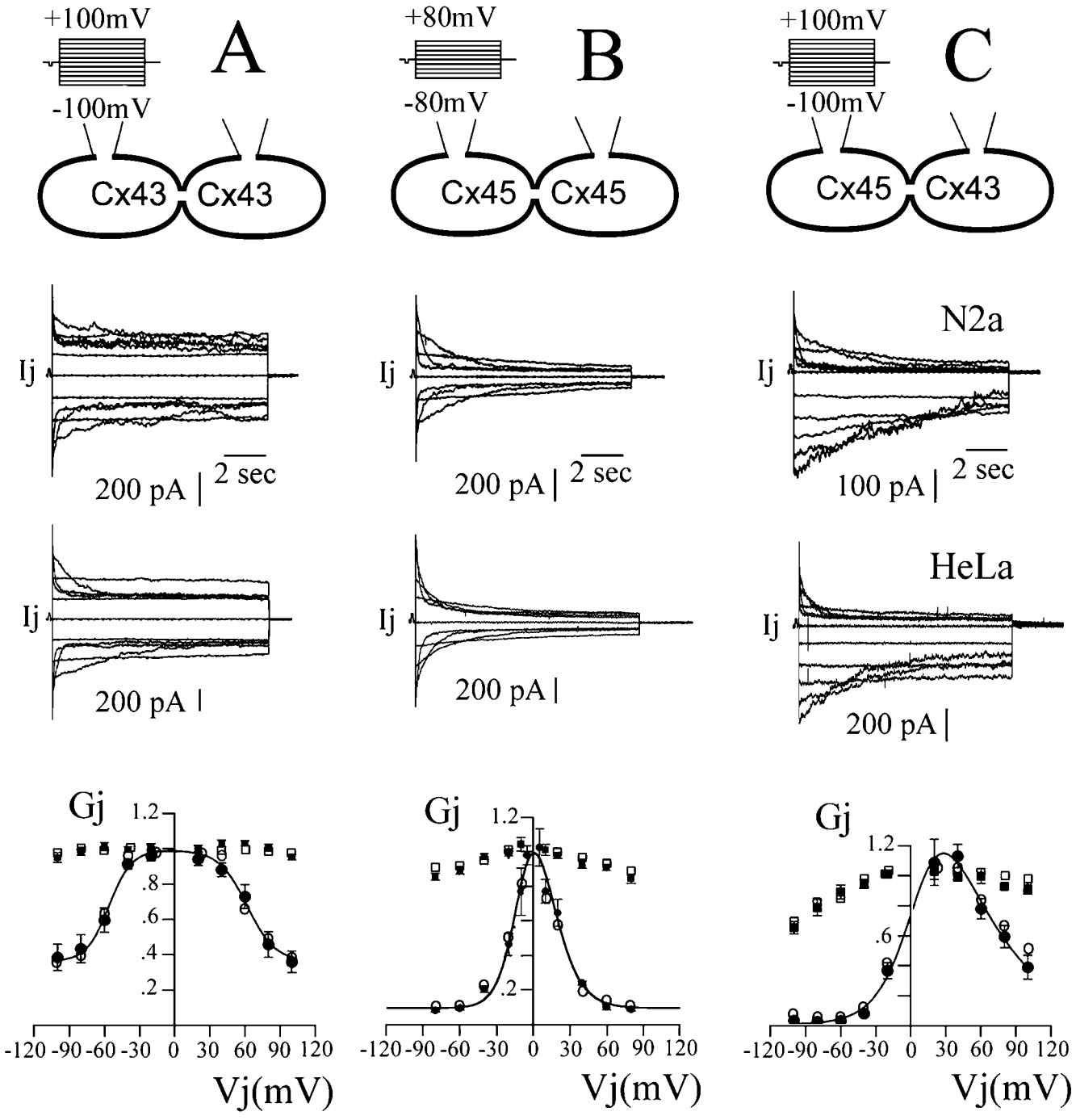

FIGURE 3 Macroscopic voltage dependence of homotypic Cx43 (*column A*), homotypic Cx45 (*column B*), and heterotypic Cx45-Cx43 (*column C*) gap junctions. All three columns contain a diagram representing the connexon pairing (*top*), original representative current traces (*middle*), and conductance versus voltage plots for the initial conductance (G_i; □ and ■) and steady-state conductance (G_{ss}; ○ and ●) obtained during a protocol of hyper- and depolarizing pulses from 100 to −100 mV. Solid and open symbols correspond to results from N2A and HeLa cells, respectively. Homotypic Cx43 channels are presented in column A, where both cells of the pairs studied expressed rCx43. The top set of traces corresponds to a representative experiment of an N2A cell pair expressing rCx43. The bottom set of traces corresponds to a representative single HeLa cell pair expressing rCx43. The plot at the bottom represents the averaged G_i (□ and ■) and G_{ss} (○ and ●) calculated from the five N2A cell pairs (■ and ●). The best fit for G_{ss} in all plots was obtained using a model developed by Chen-Izu et al. (2001) where the parameters to best fit Boltzmann curves for both polarities can be obtained simultaneously. Those parameters are shown in Table 1. Column B corresponds to cell pairs expressing homotypic Cx45 channels. The top set of current traces corresponds to an N2A/mCx45 cell pair. The bottom set corresponds to a HeLa cell pair expressing chCx45. In column C, data were obtained from cell pairs where one cell expressed Cx45, and the other Cx43. Voltage pulses were applied to the cell expressing mCx45. Cells were identified after staining each type of cell with a different fluorescent color (see Materials and Methods). The top set of traces correspond to an N2A cell pair and the bottom set to a HeLa cell pair.

TABLE 1 Transjunctional voltage-gating properties of homomultimeric and heterotypic rCx43 and mCx45 gap junction channels

		V_o (mV)			A (1/mV)		q (meV)	
	N	Negative	Positive	G_{min} (%)	Negative	Positive	Negative	Positive
mCx45	10	10.5 ± 1.4	11.9 ± 1.7	9.6 ± 0.03	0.112 ± 0.01	0.081 ± 0.010	−2.86	−2.08
rCx43	9	56.7 ± 1.8	63.1 ± 2.1	38.0 ± 0.2	0.127 ± 0.031	0.101 ± 0.021	−3.25	−2.59
mCx45-rCx43	7	1.6 ± 3.1	62.3 ± 2.8	1.8 ±0.2	0.072 ± 0.01	0.033 ± 0.003	−1.84	−0.84

All data are presented for experiments where voltage pulses were applied to the cell expressing mCx45. Fitting of all data was performed using Eq. 1. A is a constant that equals nq/kT and reflects the voltage sensitivity of the transitions between two conductive states. q represents the charge (electron mV) necessary to move against the potential. G_{max} was considered 1.0 for homotypic rCx43 and 1.6 for all fits including mCx45. The latter value was obtained because of the maximal conductance during depolarizing protocols to obtain transmembrane voltage dependency (Elenes and Moreno, 1998).

cantly slower in heterotypic channels, in particular at V_j = 60 mV.

In contrast, inactivation of Cx43 was substantially slower in heterotypic combinations when compared with homotypic Cx43 (Fig. 4 *A*). The fast inactivation time constant observed for rCx43 connexons in homotypic rCx43-rCx43 disappeared, and a significantly slower time constant was present in heterotypic rCx43 hemi-channels (Fig. 4, *A* and *C*). This was clearly reflected in the fitting of current traces. Homotypic Cx43 inactivation was fit with two exponentials, whereas heterotypic Cx43 fit well with only one exponential. An important effect of heterotypic docking was that during prolonged pulses, the inactivation of the junctional current reached values close to zero, suggesting that the non-voltage-dependent residual state was no longer present (Elenes et al., 2000). This was highlighted in the trace in the top right inset, where the current of the heterotypic channel reaches zero during the application of ±100-mV voltage pulses for 30 s. As shown below, this observation was confirmed at the single-channel level.

Microscopic current measurements from homotypic and heterotypic channels

Homotypic mCx45 unitary conductances

Single-channel recordings from N2A cells expressing mCx45 are presented in Fig. 5 *A*. The maximal single-channel conductance was determined using mainly low transjunctional voltage protocols (<60 mV). The unitary conductance values for mCx45 in transiently and stably transfected N2A cells were obtained from 15 cell pairs where multiple single-current events were measured at different voltages and grouped in the histogram included in Fig. 5 *A*. The Gaussian fit for the event histogram obtained from these experiments revealed a peak at 38 ± 5 pS (~400 events). This portion of the original trace displays a transition that did not reach a complete closed state where I_j = 0 (inset). This open state has been reported as the residual state of Cx45. The best Gaussian fit for the all-points histogram representing the main open state of the channel is shown at the right of the

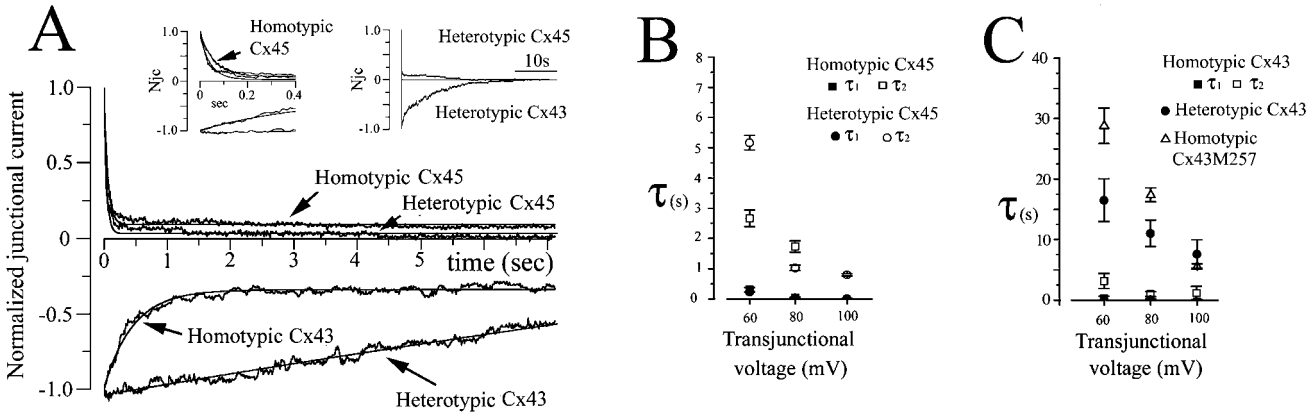

FIGURE 4 Heterotypic assembly of mCx45 and rCx43 differentially alters the gating of their constituent homomeric connexons. (*A*) Comparison of gating kinetics from junctional currents obtained from homotypic and heterotypic cell pairs during a voltage pulse of ±80 mV. Traces from these experiments were normalized to the initial conductance (G_i). (*Inset top left*) First 400 ms of current inactivation to show changes in time constants between homotypic and heterotypic channels; (*Inset top right*) Current inactivation of heterotypicCx43 during a 100-mV pulse of 30 s. (*B*) Inactivation time constants for homotypic mCx45 and heterotypic rCx43-mCx45 channels. The mCx45 connexons forming homotypic channels with mCx45 or heterotypic channels with rCx43 have comparable fast time constants (■ and ●), but the slow inactivation time constant σ_2 increased significantly (compare □ with ○). (*C*) Inactivation time constants for homotypic and heterotypic rCx43 connexons. Those connexons that form heterotypic channels with homomeric mCx45 connexons have a single and much slower kinetics of inactivation when compared with those forming homotypic rCx43-rCx43 (■ and □). These slow kinetics are comparable to those obtained from homotypic Cx43M257 (△).

amplified trace. Using the mean value of these peaks, we calculated a unitary conductance of 38 ± 4 pS and a residual of 4 pS.

Homotypic rCx43 unitary conductances

The activity of single channels formed by rCx43 in N2A cells was examined during the recovery from 2 mM halothane. Multiple openings were detected with distinct conductance levels (indicated by dashed lines in Fig. 5 *B* with the closed state for all channels ($I_j = 0$) represented by a continuous line). After the first opening, the channel entered a sub-conductance level, as has been previously described for Cx43 channels (Moreno et al., 1994a). Later, the channel closed completely, followed by consecutive openings denoting the presence of various channels becoming active. The best Gaussian fit of an all-points histogram of the digitized current (Fig. 5 *B*, right side) revealed seven clearly separate peaks and one sub-state. According to this current trace, the unitary conductances were between 119 and 121 pS with a mean and SD of 120 ± 30 pS. The event histogram on top shows the distribution of conductances from traces obtained from two cell pairs, calculated during long transjunctional voltage steps of ±40 mV. More than 500 events were measured. The best Gaussian fit yielded a γ_j of 115 ± 15 pS.

Heterotypic rCx43-mCx45 unitary conductances

The formation of heterotypic channels from rCx43 and mCx45 connexons in N2A cells yielded new conductance levels recorded in all cell pairs studied ($n = 30$). As shown in Fig. 5 *C*, these channels behave differently. We could not detect a residual conductance or any other sub-state in any of our recordings. The best Gaussian fit for an all-point histogram is shown on top of the transjunctional current trace. The unitary conductances calculated correspond to values between 55 and 65 pS. The event histogram at the right corresponds to the distribution of 300 events measured using transjunctional current traces from eight different cell pairs where the cell expressing Cx45 was stimulated with 70- and 30-mV voltage pulses of both polarities. The best Gaussian fit for this distribution corresponds to a mean unitary conductance of 58 ± 8 pS. Considering that the conductance for each homomeric connexon is twofold larger than the conductance of the homotypic channel, the resulting unitary conductance for the heterotypic channel closely corresponded to the ohmic sum of the predicted individual connexon conductances.

Unitary conductances are independent of transjunctional voltage

The unitary conductance of homotypic Cx45, Cx43, and heterotypic Cx45-Cx43 channels was independent of voltage, as is shown in Fig. 6 *A* where the ohmic behavior of these channels was revealed by the linear relationship between unitary current and voltage. Each point represents the mean and SD of the Gaussian best fit of more than 100 events for each voltage and for each channel type in three different cell pairs. These events were obtained mainly at steady state during the application of long voltage pulses. The slope for the best linear fit for mCx45 channels was 37 ± 5 pS. For Cx43, the slope represented a conductance of 121 ± 8 pS whereas heterotypic channels produced a conductance of 61 ± 5 pS.

An example of the behavior of heterotypic channels in a cell pair with few channels present is shown in Fig. 6 *B*. Here we show two transjunctional current traces obtained after stimulating the cell expressing Cx45 with ±40-mV pulses. The dashed lines indicate the conductance level of 60 pS. In the top trace, where a 40-mV pulse of negative polarity was applied, we observe a large spike at the initiation of the pulse, indicating that two channels were open. After a few milliseconds, these two channels close, and the transjunctional current is reduced to zero (solid line). The lower trace shows the transjunctional current during a 40-mV pulse obtained from the same cell pair, but recorded 20 s later. Note that two channels with identical unitary conductances are active. The open time of the channels at this polarity is substantially larger compared with the previous recording. This reduction in open time was observed with increments in the voltage steps (not shown), suggesting that, as in the homotypic channels, the gating kinetic parameters are voltage dependent.

Another clear characteristic of heterotypic channels is that the fast gating of the channels takes them to a completely closed stated, where no residual conductance was observed in any of our recordings.

To determine whether the unitary conductance was independent of the transjunctional voltage, we applied a ramp voltage protocol, as shown in Fig. 6 *C*. The top trace corresponds to homotypic Cx45 channels in N2A cells. Here, two channels were active during the voltage protocol that went from −50 to +50 mV. The slopes of these two channels along the voltage ramp yielded conductances of 38 and 40 pS and were linear throughout the whole voltage range. At the end of the trace, the residual conductance in the channels is indicated with an arrow. The bottom trace of Fig. 6 *C* corresponds to a trace obtained from heterotypic Cx43-Cx45 channels. Here, three active channels were present in the junction, and the change in unitary current was linear during the whole voltage range from −100 to +100 mV. The unitary conductances for these channels, according to the best-fitted slopes were 61, 55, and 58 pS.

Gating of heterotypic rCx43-rCx43M257

The slow gating of Cx43 connexons in heterotypic Cx43-Cx45 channels suggested that their fast voltage-gating

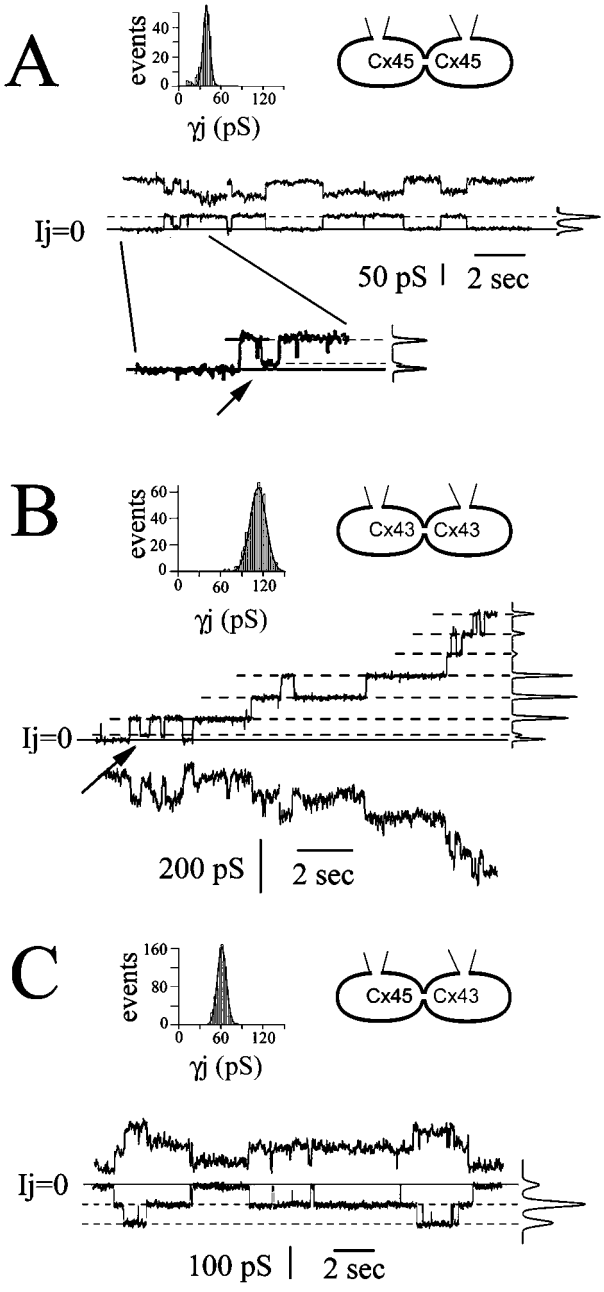

FIGURE 5 Single-channel conductance of homotypic and heterotypic gap junction channels formed by mCx45 and rCx43. Representative unitary currents are shown in all panels, including the all-points histogram for every junctional current trace. Event histograms for four to six experiments are on top together with a cell pair diagram indicating the connexins expressed. (*A*) Single-channel conductance of cell pairs expressing homotypic mCx45. The initial part of the curve was amplified to show the presence of the residual state. The event histogram represents 400 events from 15 experiments recorded at transjunctional voltages of −40 and +40 mV. The best Gaussian fit for these distributions could be obtained if γ_j = 38 ± 5. (*B*) Single-channel conductance of homogeneous gap junction channels from cell pairs expressing rCx43. The event histogram contains 570 events from two cell pairs where channel transitions were uniform in size. Gaussian best fit represents 115 ± 15 pS. All-point histogram shown at the right of the current trace yielded a unitary conductance of 120 ± 30 pS. (*C*) Single-channel conductance of heterotypic channels. The representative currents clearly show an absence of a residual state, even at large voltages. γ_j from the all-point histogram shown immediately at the right of the transjunctional trace yielded a γ_j value of 60 pS and was obtained at 60 mV. The event histogram on the right indicates that the channels had a unitary conductance of 58 ± 8 pS. Represented are 350 events from eight different cell pairs where the transjunctional voltage was from ±30 to ±70 mV and was applied at both polarities to the cell that expressed Cx45.

mechanism was impaired after docking. An alternative explanation was that Cx43 connexons gated with a polarity opposite to that of Cx45 connexons. Comparing the voltage-dependent parameters between Cx45 and Cx43 (Fig. 3), it is clear that Cx45 gates to negative voltages. Although it has been suggested that connexons constructed from either of these connexins gate to similar polarities (B. J. Nicholson, SUNY at Buffalo, personal communication), hypotheses have also been made that the gating polarity of Cx43 may change, depending on the system used. Therefore, we decided to test whether the polarity of voltage gating to which the Cx43 hemichannel is sensitive is the same as that of Cx45 in our cellular system. We performed experiments where Cx43 was forced to pair against Cx43M257, a mutant where most of the COOH terminal has been removed, together with the fast component for voltage-dependent inactivation (Revilla et al., 1999; Elenes et al., 2000). These experiments were expected to help determine whether the slow kinetics of closing the Cx43 hemichannel in heterotypic configuration is a slow component of the normal voltage gating seen in homomeric Cx43 channels or whether it represents a different kind of gating (sensitive to the other polarity of voltage), normally masked by the gating of the opposing hemichannel.

As shown in Fig. 7 *A*, homotypic Cx43M257 channels were still sensitive to voltage but showed slower gating kinetics. In fact, for V_j larger than 60 mV, current inactivation did not reach a steady state even after 10 s.

When connexons formed by Cx43M257 were paired against Cx43, the current traces showed rectification (Fig. 7 *B*). The voltage pulses that correspond to Fig. 7 *B* were applied from −100 to +100 on cells expressing Cx43M257, as shown in the cell diagram on top. The current traces indicate that Cx43 and Cx43M257 maintained their gating kinetics and, more importantly, that Cx43 gated to negative voltage, in the same way as Cx45 connexons.

Recordings at a single-channel level revealed that the residual conductance of homotypic Cx43M257 channels was not present, as it was shown for heterotypic $Cx43_{hetCx45}$. As presented in Fig. 7 *C*, the gating activity of these homotypic Cx43M257 channels showed transitions between the open and closed states, but the residual conductance was never present during recordings of 16 different cell pairs.

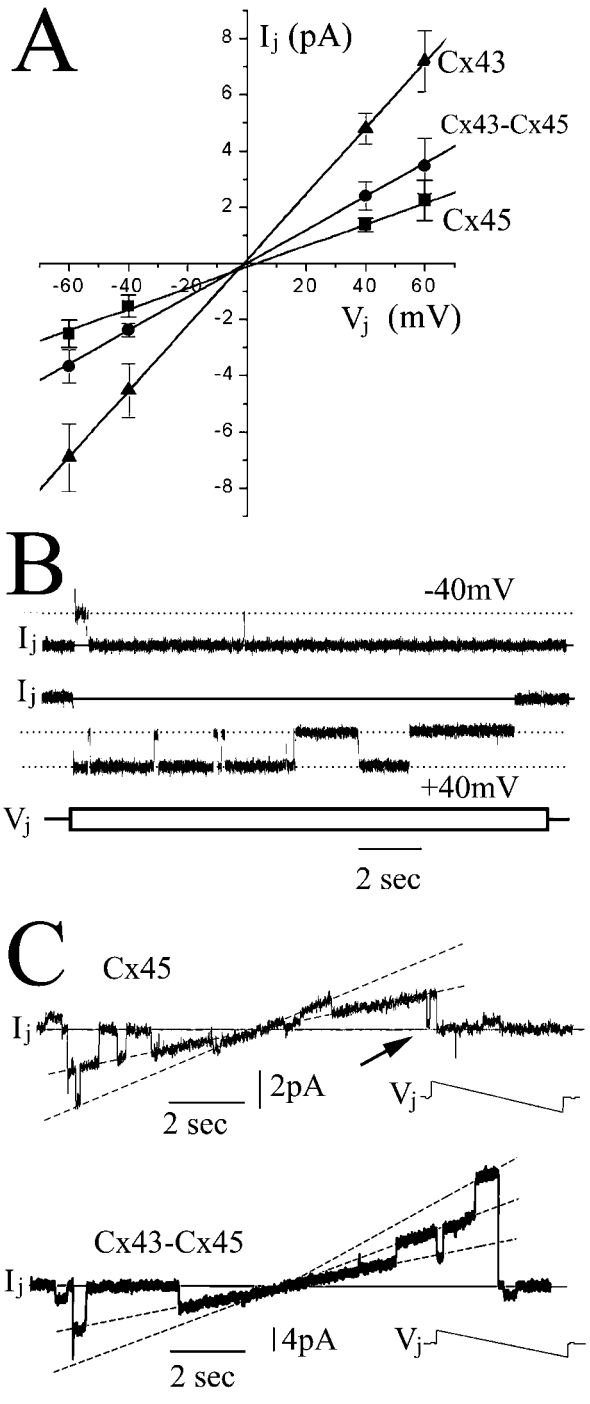

FIGURE 6 Ohmic behavior of homotypic and heterotypic channels. (*A*) The unitary conductance calculated for cell pairs with different connexin content was calculated using event histograms at distinct voltages. The mean and SE was plotted to determine the behavior of each channel type. The linear best fit for each combination corresponds to 121 ± 8 pS (rCx43-rCx43), 61 ± 5 pS (rCx43-mCx45), and 37 ± 5 pS (mCx45-mCx45). (*B*) Digitized single-channel recordings from a cell pair with heterotypic channels. This is an example where we observed that the channels gate to positive and negative voltage. Independently of voltage, they conserve their unitary conductance, and no residual conductance or sub-states are observed. (*C*) Digitized current traces obtained from homotypic Cx45 (*top*) and heterotypic Cx43-Cx43 channels (*bottom*). The voltage protocol applied during these experiments was a 10-s ramp from −50 to +50 mV for Cx45 and from −100 to +100 mV for the heterotypic channels. The traces correspond to transjunctional currents digitized at 1 kHz and filtered at 300 Hz for display. The arrow indicates the presence of a residual state in homotypic Cx45 channels.

DISCUSSION

In this study, we presented evidence that homomeric connexons formed by Cx45 dock with Cx43 homomeric connexons, blocking the fast voltage-gating inactivation of Cx43. Because changes in Cx45 voltage-gating parameters were not strongly affected, it appears that Cx45 works as an inducer to change the properties of docked Cx43 channels.

Voltage-dependent gating of heterotypic rat Cx43 and murine Cx45 channels

The data, which we obtained from gating homotypic Cx43 and Cx45, are rather similar to previously published studies. In rCx43 transfected N2A cells, V_0 was −56.7 and 63.1 mV for negative and positive pulses, respectively. These numbers are similar to those reported for cells that endogenously express (predominantly) Cx43, including rat Leydig cells (±52 mV) (Perez-Armendariz et al., 1994), neonatal rat cardiocytes (±51 mV) (Valiunas et al., 1997), human vascular smooth muscle cells (±52 mV)(Moreno et al., 1993a), and SkHep1 cells stably transfected with human Cx43 (±60 mV) (Moreno et al., 1993b). The conductance that we recorded at steady state G_{ss}/G_i in transfected N2A cells was 0.38 ± 0.02, which closely corresponds to the value previously reported for hCx43 in SkHep1 cells but is somewhat higher than values reported for Cx43 by other researchers (Valiunas et al., 1997). Although it might be very difficult to determine the cause of these discrepancies, it is possible that in some of the systems where G_{min} was lower than 20%, other connexins (such as Cx45) could have been co-expressed but not detected.

For homotypic Cx45 channels, the voltage-gating parameters obtained in our study are comparable to those obtained from human Cx45 in Skhep1 cells (Moreno et al., 1995b), where V_0 = 13.5mV. The ones previously reported for chCx45 has been significantly larger, possibly because of the cell type or the fitting protocol used (Veenstra et al., 1992). More in accordance with our results is the size of the unitary conductance in human and chick (Moreno et al., 1995b; Veenstra et al., 1992) and the presence of a residual conductance, which is no greater than 10% of the initial conductance (Kwak et al., 1995).

Many connexins have been reported to exhibit instantaneous gating of their channels (Bennett et al., 1993). For homotypic combinations, we mainly observed a reduction in total conductance with homotypic Cx45 channels that occurred in less than 100 ms and led to a calculated reduc-

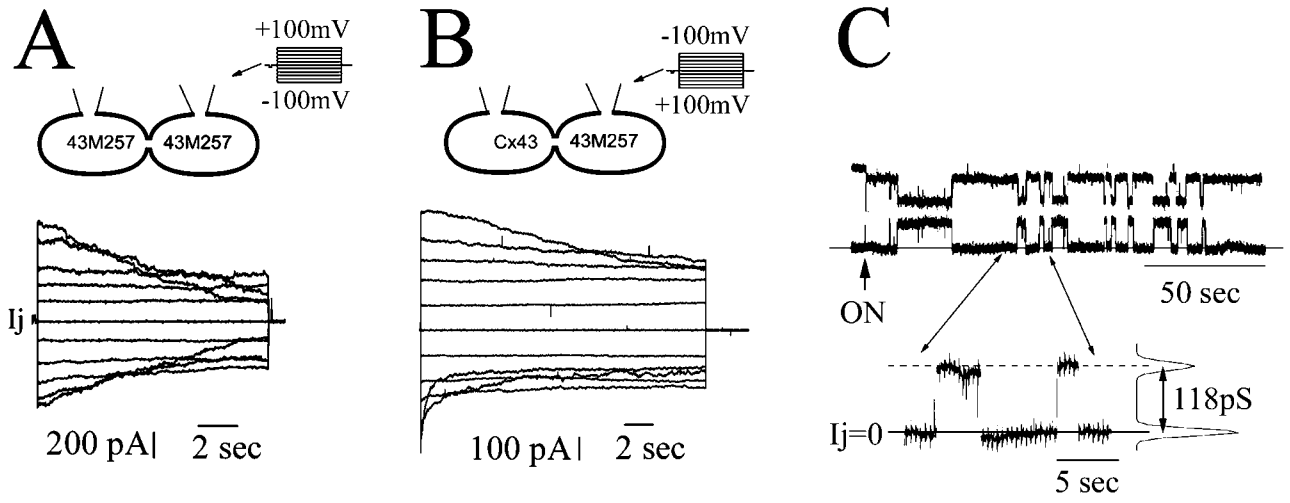

FIGURE 7 Cx43 gates to pulses of negative polarity. (*A*) At the top we show a cell pair diagram to indicate that the voltage pulses were applied to the cell on the right. Underneath is an averaged set of current traces ($n = 3$) obtained from N2A cells expressing Cx43M257, a mutant with no carboxyl tail (CT). The gating kinetics is similar to the one presented for similar polarity in heterotypic Cx45-Cx43 cell pairs (see Figs. 3 *C* and 4). (*B*) At the top, the cell diagram indicates that the voltage pulses were applied to the cell expressing Cx43M257. At the bottom there is a family of currents from those heterotypic channels formed by wild-type Cx43 and Cx43M257. These connexins form rectifying channels where the fast gating is favored when the cells expressing Cx43M257 are depolarized. (*C*) Single-channel conductance in homotypic Cx43M257 channels. The traces indicate a channel with gating activity where the state transitions go from closed to open only. The residual conductance was not observed in any of 16 cell pairs recorded. The all-point histogram on the right indicates that the channels present a unitary conductance of 118 pS, indistinguishable from that of WT Cx43 channels.

tion to 20% at ±100 mV. Because of the fast inactivation time constant, we consistently digitized currents at 5 kHz, so that the decrease in instantaneous current could be detected. This instantaneous gating became more evident in heterotypic channels, where the instantaneous reduction was as low as 40% during the application of ±80 mV and was persistent, independently of the sequence of voltage protocols applied. At a microscopic level, the unitary conductance of Cx45 is not significantly different during recordings at steady state for voltages between −60 and +60 mV, as has been reported earlier (Moreno et al., 1995b). Similar results for the same voltage range were found during our current study. Moreover, voltage ramps applied from 100 to −100 mV for homotypic Cx45 and heterotypic Cx43-Cx45 (Fig. 6 *C*) clearly indicated that there is no significant instantaneous rectification of the unitary conductance of these channels. Therefore, the instantaneous gating of these connexins is a true gating of the channels and the reduction observed in G_j-V_j curves seem to be due to lack of time resolution in our recording mechanism, more than rectification at a single-channel level.

After heterotypic docking, Cx43 and Cx45 hemichannels demonstrated different voltage-gating kinetics. In homotypic configurations, homotypic Cx43 and Cx45 channels exhibit both fast and slow inactivation. After heterotypic docking with Cx43, the fast component of Cx45 appeared to be unaffected, but the slow component became significantly slower, as calculated during 60-mV pulses. This change in kinetics occurred simultaneously with the disappearance of γ_{jres}. It remains to be elucidated how these two events are linked. On the other hand, the fast voltage-gating kinetics of the Cx43 connexon disappeared, retaining only slower kinetics that resemble those of Cx43M257. Even though the V_0 for heterotypic connexons was identical to homotypic Cx43 (63.1 vs. 62.3 mV), the gating charge significantly decreased (from 2.59 to 0.84; see Table 1 and Fig. 4), suggesting either a strong change of the gating mechanism or an involvement of a different type of gating. These observations suggest that docking of homomeric connexons formed by Cx45 and Cx43 affect both connexons, but Cx45 appears to dominate; its presence strongly blunts the voltage gating of Cx43, whereas the conductance of their connexons appears to remain unchanged (see below).

Behavior of Cx45 and Cx43 channels expressed independently and in heterotypic combination

Homotypic channels formed of Cx43 or Cx45 presented a discrete distribution of unitary conductances. The unitary conductance of mCx45 (38 pS) was only modestly larger than that determined for human Cx45 expressed in SkHep1 cells (29 pS) (Moreno et al., 1995b). Both main and residual states were present in these channels, as can be observed in Fig. 5 *A* (*arrow*) where the current in the lower trace does not reach the $I = 0$ level.

For rCx43 expressed in HeLa and N2A cells, the maximal unitary conductances found under identical conditions were

125 ± 5 (not shown) and 115 ± 5 pS (See Fig. 5 *B*), respectively. These values agree with those previously reported in other cell types (see Fig. 2 *A* in Moreno et al., 1994b). It has been consistently reported that Cx43 channels gate in response to voltage from the main open state (γ_{main}) to a sub-conductance or residual state (γ_{res}) (Bukauskas et al., 1992). The conductance of the channel at the residual state has been reported to be ~25% of the main conductance, and it is voltage insensitive (Moreno et al., 1994b). Our recordings from Cx43-Cx43 homotypic combinations are consistent with these prior observations.

Some endogenous Cx45 was detected in HeLa cells by our Western blots and electrophysiological recordings in some cell pairs. This endogenous Cx45 represented a problem with cells expressing small numbers of exogenous channels, where rectification was consistently observed; nonetheless, when the expression of exogenous connexins was high, the voltage-gating properties were consistently observed, regardless of the cell type.

When N2A cells expressing rCx43 were paired with N2A cells expressing mCx45, the resulting heterotypic Cx43-Cx45 channels had an average unitary conductance of 60 ± 7 pS that was not dependent on voltage (see Figs. 5 and 6). The observed value for the heterotypic channel conductance ($ht\gamma_{main}$) was very close to the predicted conductance value ($c\gamma_{main}$ = 59 pS) for homomeric rCx43 and mCx45 connexons in series as calculated according to ($ht\gamma_{main} = 1/\{(1/c\gamma j_{mainCx43})+(1/c\gamma j_{mainCx45})\}$) if $c\gamma j_{mainCx43}$ = 260 pS and $c\gamma j_{mainCx45}$ = 76 pS). We have previously presented a similar prediction for the heterotypic docking of hCx45 and hCx43 (Moreno et al., 1995a).

Another notable characteristic of the heterotypic Cx43-Cx45 channels was that the residual conductance was not detected in any of the cell pairs recorded. Fig. 6 displays an example where the unitary channel activity was recorded at 40 mV applied in both polarities. If we consider that the residual conductance is responsible for G_{min} at the macroscopic level (Moreno et al., 1994a), when the cells are pulsed to any voltage, the gating of the heterotypic channels should be complete. This previously observed trend (Moreno et al., 1995a; Steiner and Ebihara, 1996) is represented in Fig. 3 *C* and was confirmed with single-channel recordings like the one in Fig. 6 *B*, where complete closure of channels occurred.

Voltage gating of Cx43M257 and other modified Cx43 connexons

The inactivation kinetics of Cx43 connexons in heterotypic combination with Cx45 ($Cx43_{het45}$) closely resembled those of Cx43M257. The voltage dependence calculated at the steady state (G_{min}) and the inactivation constants at 60, 80, or 100 mV produced results that were strikingly similar. Because these two completely different approaches yield similar inactivation kinetics and identical single-channel behavior, we suggest that a general gating mechanism has been eliminated through both maneuvers.

A similar elimination of fast gating has been observed when the large green fluorescent protein molecule was added to the carboxy terminal (CT) of Cx43 (Bukauskas et al., 2000), suggesting that this part of the molecule participates directly in voltage-gating inactivation. Furthermore, in experiments where CT domains of Cx43 or Cx40 were co-expressed with truncated Cx40 channels in N2A cells, the channels recovered their low-conductance state, indicating that this domain is required for the channels to maintain their residual conductance (Anumonwo et al., 2001).

Proposed mechanism for alterations in gating of Cx43 connexins in heterotypic combination with Cx45

Available data from various laboratories clearly implicate the CT domain in the fast inactivation of Cx43 connexons. The CT domain may act directly as the molecular region that plugs the channel, or it may induce another region of the channel to undergo a conformational change that partially closes the channel. Currently, we cannot differentiate among these possibilities, but we know that when the tail is present in Cx43 connexons, the conformational change that completely closes the channel cannot occur; therefore, the channel reaches a residual conductive state. However, if the CT tails are removed (Cx43M257), the channel can now go through a conformational change that favors complete closure with slow kinetics. It has been suggested that this slow gating in wild-type channels is hindered by the fast gating of the channel (Revilla et al., 1999). One candidate for this slow inactivation is the loop gating described initially in functional hemichannels (Trexler et al., 1996) and possibly related to chemical gating (Bukauskas and Peracchia, 1997); its origin is yet to be determined.

According to our results, heterotypic docking has affected both connexons. The most striking features are 1) the changes of fast gating of Cx43 that resemble the voltage gating of Cx43 lacking its CT and 2) the loss of residual conductance for both Cx43 and Cx45 connexons. Our data show no substantial changes in the unitary conductance of the channel. The main changes have occurred at the level of particle-receptor interaction, as suggested for other connexins (Anumonwo et al., 2001). Whether this is due to a change in the receptor region or in the CT remains to be elucidated.

Currently the initial model from Revilla et al. (1999), where CT acts as a ball that interacts with a channel, seems to be the most appropriate explanation for our results. One objection to this model is that it was generated after the removal of a portion of the protein, which could have generated other effects on the remaining portions of the connexin. With our experimental data, we have now confirmed, without any mutation, that the fast gating mecha-

nism of Cx43 can be modulated by heterotypic docking that produces similar effects to those seen in the mutated connexin, including the elimination of fast gating and the appearance of stronger slow gating. Clearly, these experiments strongly suggest that the two gating mechanisms can remain independent, even in the presence of CT. Therefore, we suggest that under transjunctional voltage, the heterotypic channel will try to go through a conformational change to close completely, but this closure can be accomplished only if the whole channel becomes altered after docking and the CT of Cx43 does not hinder this closure. If the transjunctional voltage pulse is applied with reverse polarity, the time constant for Cx45 is reduced (see Fig. 4), meaning that this gate closes faster, possibly because the absence of the Cx43 tail on the other side favors configuration of the channel into the closed state. The molecular mechanism(s) involved in the inhibition of the fast gating of Cx43 caused by docking with Cx45 remains to be investigated.

Functional significance

Cardiac cells express at least three connexins (Cx43, Cx40, and Cx45). Although the properties of channels formed of each of these connexins may contribute to the properties of cardiac tissues, the formation of heterotypic junctions within the heart (as has been demonstrated by Elenes et al., 1999) would provide an additional method for regulating intercellular communication. Each cardiac connexin has its own biophysical properties (including voltage dependence, selectivity, and unitary conductance) as has been demonstrated by studying each connexin individually. Because Cx45 has one of the smallest conductances, it might exert an antagonistic effect on rapid conduction in the cardiac fibers where this connexin is expressed or even a reduction in metabolic communication as has been reported previously (Steinberg et al., 1994; Koval et al., 1995).

We have observed changes in fast voltage gating in heterotypic Cx43-Cx45, which may involve the Cx43 CT. This domain is also involved in pH dependence and includes various phosphorylation sites; therefore, heterotypic interactions of cardiac connexins might also influence channel regulation in response to other factors such as protein kinases or cytoplasmic acidification. It has been shown that Cx43 and Cx45 respond to protein kinase C activation by a reduction of their unitary conductance (Moreno et al., 1992, 1994b; Kwak et al., 1995) or their open probability (vanVeen et al., 2000). In contrast, Cx40 responds to protein kinase A by an increase in its unitary conductance (van Rijen et al., 1998). It is not known whether heterotypic channels are more or less prone to gate after being phosphorylated by different kinases. Individually, Cx45 channels are more pH sensitive than Cx43 channels (Hermans et al., 1995); thus, pairing of Cx45 with Cx43 might also alter pH gating.

In summary, the data we have presented support the idea that new conduction and gating properties of channels become evident when cells form heterotypic channels (such as between Cx45 and Cx43). Without using site-directed mutagenesis, we demonstrated that the gating of Cx43 heterotypic connexons resemble those of homotypic connexons formed by Cx43 lacking the CT. This effect strongly suggests that heterotypic interaction has impaired the fast gating mechanism. Simultaneously with this loss of fast gating properties, heterotypic channels gate from closed to open state without a residual conductance, demonstrating that these two events are correlated. The presence of functional heterotypic channels in cardiac myocytes, or in other cells that express two or more different connexins, would enable not only conductive steady-state differences but also an alteration in the gating responsiveness of the cells.

We thank Dr. Steve Taffet for allowing us to use the Cx43M257 transfected cells. We thank also Patricia L. Mantel for her technical and writing assistance.

This work was supported by National Institutes of Health grants HL63969 and HL50485 to A.P.M. and HL59199 and HD09402 to E.C.B.

REFERENCES

Anumonwo, J. M., S. M. Taffet, H. Gu, M. Chanson, A. P. Moreno, and M. Delmar. 2001. The carboxyl terminal domain regulates the unitary conductance and voltage-dependence of connexin40 gap junction channels. *Circ. Res.* 88:666–673.

Barrio, L. C., J. Capel, J. A. Jarillo, C. Castro, and A. Revilla. 1997. Species-specific voltage-gating properties of connexin-45 junctions expressed in *Xenopus* oocytes. *Biophys. J.* 73:757–769.

Bennett, M. V., J. B. Rubin, T. A. Bargiello, and V. K. Verselis. 1993. Structure-function studies of voltage sensitivity of connexins, the family of gap junction forming proteins. *Jpn. J. Physiol.* 43:S301–S310.

Berthoud, V., P. Tadros, and E. Beyer. 2000. Connexin and gap junction degradation. *Methods Enzymol.* 20:180–187.

Beyer, E. C. 1990. Molecular cloning and developmental expression of two chick embryo gap junction proteins. *J. Biol. Chem.* 265:14439–14443.

Beyer, E. C., D. L. Paul, and D. A. Goodenough. 1987. Connexin43: a protein from rat heart homologous to a gap junction protein from liver. *J. Cell Biol.* 105:2621–2629.

Bradford, M. M. 1976. A rapid and sensitive method for the quantitation of microgram quantities of protein using the principle of protein-dye binding. *Anal. Biochem.* 72:248–254.

Bukauskas, F. F., K. Jordan, A. Bukauskiene, M. V. Bennett, P. D. Lampe, D. W. Laird, and V. K. Verselis. 2000. Clustering of connexin 43-enhanced green fluorescent protein gap junction channels and functional coupling in living cells. *Proc. Natl. Acad. Sci. U.S.A.* 97:2556–2561.

Bukauskas, F., C. Kempf, and R. Weingart. 1992. Electrical coupling between cells of the insect *Aedes albopictus*. *J. Physiol.* 448:321–337.

Bukauskas, F. F., and C. Peracchia. 1997. Two distinct gating mechanisms in gap junction channels: CO_2- sensitive and voltage-sensitive. *Biophys. J.* 72:2137–2142.

Burt, J. M., and D. C. Spray. 1989. Volatile anesthetics block intercellular communication between neonatal rat myocardial cells. *Circ. Res.* 65: 829–837.

Chen-Izu, Y., A. P. Moreno, and R. A. Spangler. 2001. A two opposing gates model for the asymmetric voltage gating of gap junction channels. *Am. J. Physiol.* In press.

Coppen, S. R., E. Dupont, S. Rothery, and N. J. Severs. 1998. Connexin45 expression is preferentially associated with the ventricular conduction system in mouse and rat heart. *Circ. Res.* 82:232–243.

Crow, D. S., E. C. Beyer, D. L. Paul, S. S. Kobe, and A. F. Lau. 1990. Phosphorylation of connexin43 gap junction protein in uninfected and Rous sarcoma virus-transformed mammalian fibroblasts. *Mol. Cell Biol.* 10:1754–1763.

Ek-Vitorin, J. F., G. Calero, G. E. Morley, W. Coombs, S. M. Taffet, and M. Delmar. 1996. pH regulation of connexin43: molecular analysis of the gating particle. *Biophys. J.* 71:1273–1284.

Elenes, S., M. Chanson, and A. P. Moreno. 2000. The carboxyl-terminal of connexin43 modulates channels' unitary conductance distribution and their voltage gating kinetics. *Biophys. J.* 78:319a.

Elenes, S., M. H. Rubart, and A. P. Moreno. 1999. Junctional communication between isolated pairs of canine atrial cells is mediated by homogeneous and heterogeneous gap junction channels. *J. Cardiovasc. Electrophys.* 10:990.

Elenes, S., and A. P. Moreno. 1998. Murine Cx45: voltage dependence characterization at physiological conditions. *Mol. Biol. Cell.* 9:95a.

Gros, D. B., and H. J. Jongsma. 1996. Connexins in mammalian heart function. *Bioessays.* 18:719–730.

Haefliger, J. A., R. Polikar, G. Schnyder, M. Burdet, E. Sutter, T. Pexieder, P. Nicod, and P. Meda. 2000. Connexin37 in normal and pathological development of mouse heart and great arteries. *Dev. Dynam.* 218: 331–344.

Hennemann, H., H. J. Schwarz, and K. Willecke. 1992. Characterization of gap junction genes expressed in F9 embryonic carcinoma cells: molecular cloning of mouse connexin31 and -45 cDNAs. *Eur. J. Cell. Biol.* 57:51–58.

Hermans, M. M., P. Kortekaas, H. J. Jongsma, and M. B. Rook. 1995. pH sensitivity of the cardiac gap junction proteins, connexin 45 and 43. *Pflugers. Arch.* 431:138–140.

Kanter, H. L., J. G. Laing, E. C. Beyer, K. G. Green, and J. E. Saffitz. 1993. Multiple connexins colocalize in canine ventricular myocyte gap junctions. *Circ. Res.* 73:344–350.

Koval, M., S. T. Geist, E. M. Westphale, A. E. Kemendy, R. Civitelli, E. C. Beyer, and T. H. Steinberg. 1995. Transfected connexin45 alters gap junction permeability in cells expressing endogenous connexin43. *J. Cell Biol.* 130:987–995.

Kwak, B. R., M. M. Hermans, H. R. De Jonge, S. M. Lohmann, H. J. Jongsma, and M. Chanson. 1995. Differential regulation of distinct types of gap junction channels by similar phosphorylating conditions. *Mol. Biol. Cell.* 6:1707–1719.

Moreno, A. P., A. C. Campos de Carvalho, G. Christ, A. Melman, and D. C. Spray. 1993a. Gap junctions between human corpus cavernosum smooth muscle cells: gating properties and unitary conductance. *Am. J. Physiol.* 264:C80–C92.

Moreno, A. P., B. Eghbali, and D. C. Spray. 1991. Connexin32 gap junction channels in stably transfected cells: equilibrium and kinetic properties. *Biophys. J.* 60:1267–1277.

Moreno, A. P., G. I. Fishman, E. C. Beyer, and D. C. Spray. 1995a. Voltage dependent gating and single channel analysis of heterotypic gap junction channels formed of Cx45 and Cx43. *In* Intercellular Communication through Gap Junctions. Y. Kanno, K. Kataoka, Y. Shiba, Y. Shibata, and T. Shimazu, editors. Elsevier Science, Amsterdam. 405–408.

Moreno, A. P., G. I. Fishman, B. Eghbali, and D. C. Spray. 1993b. Unmasking electrophysiological properties of connexins32 and 43: transfection of communication-deficient cells with wild type and mutant connexins. *Prog. Cell Res.* 3:127–132.

Moreno, A. P., G. I. Fishman, and D. C. Spray. 1992. Phosphorylation shifts unitary conductance and modifies voltage dependent kinetics of human connexin43 gap junction channels. *Biophys. J.* 62:51–53.

Moreno, A. P., J. G. Laing, E. C. Beyer, and D. C. Spray. 1995b. Properties of gap junction channels formed of connexin 45 endogenously expressed in human hepatoma (SKHep1) cells. *Am. J. Physiol.* 268:C356–C365.

Moreno, A. P., M. B. Rook, G. I. Fishman, and D. C. Spray. 1994a. Gap junction channels: distinct voltage-sensitive and -insensitive conductance states. *Biophys. J.* 67:113–119.

Moreno, A. P., J. C. Saez, G. I. Fishman, and D. C. Spray. 1994b. Human connexin43 gap junction channels: regulation of unitary conductances by phosphorylation. *Circ. Res.* 74:1050–1057.

Musil, L. S., E. C. Beyer, and D. A. Goodenough. 1990. Expression of the gap junction protein connexin43 in embryonic chick lens: molecular cloning, ultrastructural localization, and post-translational phosphorylation. *J. Membr. Biol.* 116:163–175.

Paul, D. L., L. Ebihara, L. J. Takemoto, K. I. Swenson, and D. A. Goodenough. 1991. Connexin46, a novel lens gap junction protein, induces voltage- gated currents in nonjunctional plasma membrane of *Xenopus* oocytes. *J. Cell Biol.* 115:1077–1089.

Perez-Armendariz, E. M., M. C. Romano, J. Luna, C. Miranda, M. V. Bennett, and A. P. Moreno. 1994. Characterization of gap junctions between pairs of Leydig cells from mouse testis. *Am. J. Physiol.* 267: C570–C580.

Reed, K. E., E. M. Westphale, D. M. Larson, H. Z. Wang, R. D. Veenstra, and E. C. Beyer. 1993. Molecular cloning and functional expression of human connexin37, an endothelial cell gap junction protein. *J. Clin. Invest.* 91:997–1004.

Revilla, A., C. Castro, and L. C. Barrio. 1999. Molecular dissection of transjunctional voltage dependence in the connexin-32 and connexin-43 junctions. *Biophys. J.* 77:1374–1383.

Steinberg, T. H., R. Civitelli, S. T. Geist, A. J. Robertson, E. Hick, R. D. Veenstra, H. Z. Wang, P. M. Warlow, E. M. Westphale, J. G. Laing, and E. C. Beyer. 1994. Connexin43 and connexin45 form gap junctions with different molecular permeabilities in osteoblastic cells. *EMBO J.* 13: 744–750.

Steiner, E., and L. Ebihara. 1996. Functional characterization of canine connexin45. *J. Membr. Biol.* 150:153–161.

Traub, O., R. Eckert, H. Lichtenberg-Frate, C. Elfgang, D. F. Hulser, K. Willecke, B. Bastide, and K. H. Scheidtmann. 1994. Immunochemical and electrophysiological characterization of murine connexin40 and -43 in mouse tissues and transfected human cells. *Eur. J. Cell Biol.* 64:101–112.

Trexler, E. B., M. V. Bennett, T. A. Bargiello, and V. K. Verselis. 1996. Voltage gating and permeation in a gap junction hemichannel. *Proc. Natl. Acad. Sci. U.S.A.* 93:5836–5841.

Valiunas, V., F. F. Bukauskas, and R. Weingart. 1997. Conductances and selective permeability of connexin43 gap junction channels examined in neonatal rat heart cells. *Circ. Res.* 80:708–719.

van Rijen, H., M. Hermans, H. J. Jongsma, and M. Rook. 1997. Human connexin40 gap junction channels are modulated by cAMP. Proc. Int. Gap Junction Conf., Key Largo, FL. 98-99.

vanVeen, T. A. B., H. V. M. vanRijen, and H. J. Jongsma. 2000. Electrical conductance of mouse connexin45 gap junction channels is modulated by phosphorylation. *Cardiovasc. Res.* 46:496–510.

Veenstra, R. D., H. Z. Wang, D. A. Beblo, M. G. Chilton, A. L. Harris, E. C. Beyer, and P. R. Brink. 1995. Selectivity of connexin-specific gap junctions does not correlate with channel conductance. *Circ. Res.* 77: 1156–1165.

Veenstra, R. D., H. Z. Wang, E. M. Westphale, and E. C. Beyer. 1992. Multiple connexins confer distinct regulatory and conductance properties of gap junctions in developing heart. *Circ. Res.* 71:1277–1283.

Wang, X. G. and C. Peracchia. 1998. Chemical gating of heteromeric and heterotypic gap junction channels. *J. Membr. Biol.* 162:169–176.

Werner, R., E. Levine, C. Rabadan Diehl, and G. Dahl. 1989. Formation of hybrid cell-cell channels. *Proc. Natl. Acad. Sci. U.S.A.* 86:5380–5384.